Structural parameters of the interaction between ciprofloxacin and human topoisomerase-II β enzyme: toward new ^{19}F NMR Chemical Shift probes

Sales, T. A.[a]; Gonçalves, M. A.[b], and Ramalho T.C.[c,d*]

[a]Department of Chemistry, Federal University of Lavras, Lavras, Brazil, ORCID ID 0000-0002-5046-188X;
[b]Department of Chemistry, Federal University of Lavras, Lavras, Brazil, ORCID ID 0000-0003-3736-648X;
[c]Department of Chemistry, Federal University of Lavras, Lavras, Brazil, ORCID ID 0000-0002-7324-1353;
[d]Department of Chemistry, Faculty of Science, University of Hradec Králové, Hradec Králové, Czech Republic.
thaissales194@hotmail.com ; teo@ufla.br

Abstract: New tools for cancer diagnosis are being studied day by day, since early diagnosis can be crucial for a successful treatment. In this context, the use of NMR probes constitutes an efficient way of diagnosis. In this work, we investigated the use of ciprofloxacin to indirectly label the overexpression of topoisomerase-II enzymes by changes in ^{19}F NMR chemical shifts of ciprofloxacin. Increased topoisomerase-II expression has been associated with cancer occurrence, mainly with aggressive forms of breast cancer, thus constituting a promising molecular target for new tumor cell identifiers. Using DFT calculations, a spectroscopy analysis of ciprofloxacin in different chemical environments, evaluating the solvent and enzymatic effects was performed. Our results point that the ciprofloxacin forms a stable complex with the enzyme, and the main intermolecular interactions between ciprofloxacin and human topoisomerase-IIβ are hydrogen bonds, following by π-π stacking and electrostatic interactions. Also, a shift of 6.04 ppm occurs in the ^{19}F NMR signal when ciprofloxacin is interacting with the human topoisomerase-IIβ enzyme, and that this parameter may be a possible indirect marker to indicate the overexpression of these enzymes in the body.

Keywords: Spectroscopic probe; computational methods; drug repositioning; cancer diagnosis

1. Introduction

Fluoroquinolones (FQ) were introduced more than 20 years ago and are a quinolone derivative class of molecules, known for their antibacterial activity [1]. The broad commercialized antibacterial agent ciprofloxacin (CPX) is one representative of the FQs[2–4]. These compounds exert antibacterial activity because of inhibition of two bacterial enzymes, DNA gyrase and topoisomerase II enzymes [5,6]. The later are considered to be the primary target of several anticancer agents, such as doxorubicin and etoposide [7–9], being under continuous investigation aiming new anticancer drugs development, once some evidences indicate increased levels of topoisomerase II in several types of proliferating cancer cells, including Gallbladder cancer [10] , aggressive breast cancer [10–12], epithelial ovarian cancer [10,13–15], lymphomas and sarcomas [16–18], colon cancer [10] and some others. Speaking more specifically about breast cancer, increased levels of this enzyme are associated with more aggressive breast cancer, being related to increased expression of the oncogene HER2 neu, being also related to predicted disease-related death, lymph node metastasis, and advanced tumor stage[19].

Currently, cancer is one of the deadliest diseases in the world [20–23], and one factor that contributes for numerous deaths is the difficulty in diagnosing[24,25]. In general, it can be considered three main aspects that influence the cancer early diagnosis, which are awareness and search for health care, clinical and diagnostic evaluation and, finally, access to treatment [26]. Regarding the latter, it is important to stress that access barriers are a problem mainly in underdeveloped countries. In developed countries, prognosis occurs in more than 70% of the cases, while in underdeveloped countries only 20-50% of the patients have an early diagnosis, which compromises the chances of cure [27]. In this sense, the research, development and implementation of fast, simple and low-cost tools can help change this reality. [28–30]. Besides all these factors, new research into diagnostic tools is aimed at developing systems that are increasingly capable of locating species in different environments, with high specificity and resolution [28,31–34]. In this sense, many spectroscopic techniques have been explored, as is the case of Nuclear Magnetic Resonance (NMR) [29,35–42]. Molecules that interact with key enzymes can act as

spectroscopic probes [43], and these molecules are of great interest, once they are highly sensitive and easy to operate, enabling its location in live systems in a fast way[44].

In CPX molecule, the presence of fluorine atom allows the application of ^{19}F NMR spectroscopy techniques. The large chemical shift range together with the high sensitivity of ^{19}F NMR nuclei makes ^{19}F NMR an extremely attractive proposition [45]. Additionally, naturally occurring fluorine compounds are scarce, and because of this, ^{19}F NMR offers an attractive option for investigating the interactions between proteins and other biomolecules, as well as structure and mechanisms of action of fluorinated inhibitors [46]. In addition to the already mentioned advantages of ^{19}F NMR, it is also worth noting that this technique is particularly useful for studying large proteins that cannot be easily probed by conventional NMR experiments [47].

Computational methods have been widely employed to predict spectroscopic properties of various compounds for various purposes [48–50]. In fact, theoretical methods offer a fast, efficient and practical way to investigate changes in the NMR properties of different compounds, which can be caused by several factors, such as changes in the chemical environment or structure of the molecule, caused by interactions with biological macromolecules [29,51]. In this context, the aim of this study is to investigate theoretically, the behavior of CPX in the human topoisomerase-II β (hTOPO-II) active site, evaluating how this interaction affects the ^{19}F NMR chemical shift of CPX to propose the use of CPX as a spectroscopic NMR probe for cancer diagnosis.

2. Methodology

2.1. Molecular dynamics simulations

The theoretical analysis performed in this work was done with the DNA topoisomerase II β enzyme. FQs is known to be DNA gyrase and topoisomerase inhibitors. However, considering that in this work the proposal is to use this drug as a NMR probe to be used in humans, and that the enzyme DNA gyrase is apparently present in bacteria, but absent in large eukaryotes [8,52,53], the authors understand that there is no need for a study also considering the interaction of ciprofloxacin with the DNA gyrase enzyme. The first MD simulation was performed with CPX in active site of hTOPO-II enzyme. Therefore, the crystallographic structure of hTOPO-II in complex with DNA (PDB-ID 5ZAD) was obtained from Protein Data Bank [54] while CPX topology and charge data were taken from the Automated Topology Builder (ATB) Repository [55]. The simulation was performed employing GROMACS® Package [56] using Gromos 54a7 force field [57]. The system CPX:hTOPO-IIβ was solvated inside a cubic box with SPC water model. The algorithm steepest descent was employed for minimization step, stopping minimization when the maximum force was under 10.0 kJ/mol. A heading step of 1 ps was performed in NVT ensemble and for equilibrium simulation in NPT ensemble, the temperature and pressure were respectively controlled by the v-rescale thermostat (300 K) and Berendsen barostat (1 bar). The last simulation step was the performance of 10 ns of MD simulation, using barostat and thermostat Parrinello-Rahman and v-rescale, respectively. Coordinates, velocities and energies were saved at 10.0 ps of simulation, obtaining 1000 frames at the end of simulation. For both steps, the leap-frog integrator was adopted.

Finally, to select the best conformations, the optimal wavelet signal compression algorithm (OWSCA) [58] was used. This algorithm is based on a wavelet compression strategy, in which an optimization algorithm is applied to compress the maximum number of wavelet coefficients, instead of using heuristically chosen parameters. A second MD simulation of free CPX in a water box (CPX:explicit

water system) was also performed under the same conditions as mentioned above for comparison of ^{19}FNMR chemical shifts.

2.2 ^{19}F NMR chemical shift (δ) calculations

All ^{19}F NMR shielding constants calculations of this step were performed using GAUSSIAN 09 software package [59] at DFT level with the B3LYP functional and Dunning basis set [60] with diffuse function [61,62] aug-cc-pVDZ, by applying gauge-including atomic orbital (GIAO) method [63]. These levels of theory selected were based on previous parametrization studies performed on NMR calculations [64] for the CPX molecule [49]. Calculations were made for CPX in the selected frames of two MD systems using the ONIOM model [65]. In CPX:explicit water system, the first solvation shell was maintained, and the obtained values were compared with the results obtained for the CPX:hTOPO-II system. Additionally, ^{19}F NMR shielding constants were calculated also for CPX in vacuum (CPX:vacuum), and using the IEF-PCM solvation model [66], employing water as solvent (CPX: implicit water). For both systems, the initial structures were generated from a conformational analysis in Spartan 14® software using molecular mechanics. After this step, the ten lowest energy conformations obtained were subjected to geometry optimization calculations in Gaussian software at B3LYP/aug-cc-pVDZ level of theory. After that, NMR calculations were performed in the same way as in the previous systems.

The theoretical ^{19}F NMR chemical shifts were calculated in ppm according to Equation (1) [64]. The chemical shifts were expressed relative to the external chemical shit reference CF_3COOH. Theoretical results obtained were compared with experimental data, where measurements were carried out using the same reference compound [67,68].

$$\delta_{teor} = \sigma_{ref}^{cal} - \sigma_{CPX}^{cal} \quad (1)$$

Where σ_{ref}^{cal} and σ_{CPX}^{cal} are the isotropic NMR shieldings of the reference compound (CF_3COOH) and the CPX frame, respectively. To analyze the agreement between theoretical values for chemical shifts and the experimental ^{19}F NMR chemical shifts data, the Δδ calculation was performed using equation 2 that follows [64]:

$$\Delta\delta = \delta_{exp} - \delta^{cal} \quad (2)$$

1. Results and Discussion

It is well known that the CPX, as all FQs, are a bacterial topoisomerase inhibitor [6,69]. However, due to the presence of these enzymes in the human body, in the last years many experimental researches have been pointed the potential of this drug and its derivatives to also inhibit human topoisomerases [12,70–76]. Recently, in order to better understand the action mechanisms and the main differences between the interactions in TOPO-II of the two organisms, some theoretical investigations have already been done [77,78]. A previous study that investigates the interaction of thirteen FQs with human topoisomerases by molecular docking studies pointed that CPX is able to perform a hydrogen bond with the hTOPO-IIβ active site aminoacid Asp 479 [79]. The found binding affinity was -9.62 kcal.mol^{-1}. Other recent theoretical investigation explored how CPX binds to different sites of the hTOPO-IIβ enzyme [77]. Also, through molecular docking calculations, the authors showed that CPX has similar interaction energy in both human and bacterial enzyme and that CPX preferentially interacts in the same local of

chemotherapeutic agent etoposide acts. The found interaction energy for CPX in aforementioned study was -71.62 kcal.mol^{-1} and CPX was able to perform hydrogen bonds with Glu477, Tyr 821, Gln778, and Asp 479 amino acid residues.

All the mentioned researches above use the molecular docking technique in their investigations. Molecular docking is an important computational technique in structural biology and computer-aided drug design[80]. The main goal of this type of computational simulation is to evaluate the most feasible binding geometries of a ligand to a target protein whose three-dimensional structure is known [81,82]. Despite their fundamental importance in this research field, docking studies only provide a static view of the interactions between the ligand and the protein. MD simulations, on the other hand, are used to analyse the dynamic behaviour of these interactions as well as of the entire system, helping to reproduce the biological events in a computer simulation [83,84]. Here, the main proposal is to investigate the possibility of using the well-known antibiotic ciprofloxacin as a ^{19}F NMR chemical shift probe to localize the overexpression of hTPO-IIβ, which is associated with cancer incidence [10,85]. For this, a dynamic analysis of the system is of crucial importance.

1.1. MD simulations

In order to analyze the influence of the chemical environment on the conformational change of CPX, two MD simulations were performed. One simulation was done with CPX in the hTOPO-II active site (CPX:hTOPO-II system) as the other was performed with CPX only in a water box (CPX:explicit water). By the analysis of Root Mean Square Deviation (RMSD) of CPX in both systems (Figure 1), it is possible to observe that the systems reached equilibrium around 2000 ps of simulation, and this time was used as a starting time for the selection of representative frames using OWSCA algorithm. As can also be seen in Figure 1, there is a slightly higher flexibility of CPX in the aqueous system, when compared to molecule in the enzyme active site. This makes sense, once that in the active site, the molecule has greater conformational restriction because of the presence of surrounding amino acids, with which it carries out intermolecular interactions. Additionally, the RMSD levels, mainly for CPX in hTOPO-II active site, are around 0.1 nm (1Å), indicating high stability of the structures [86,87].

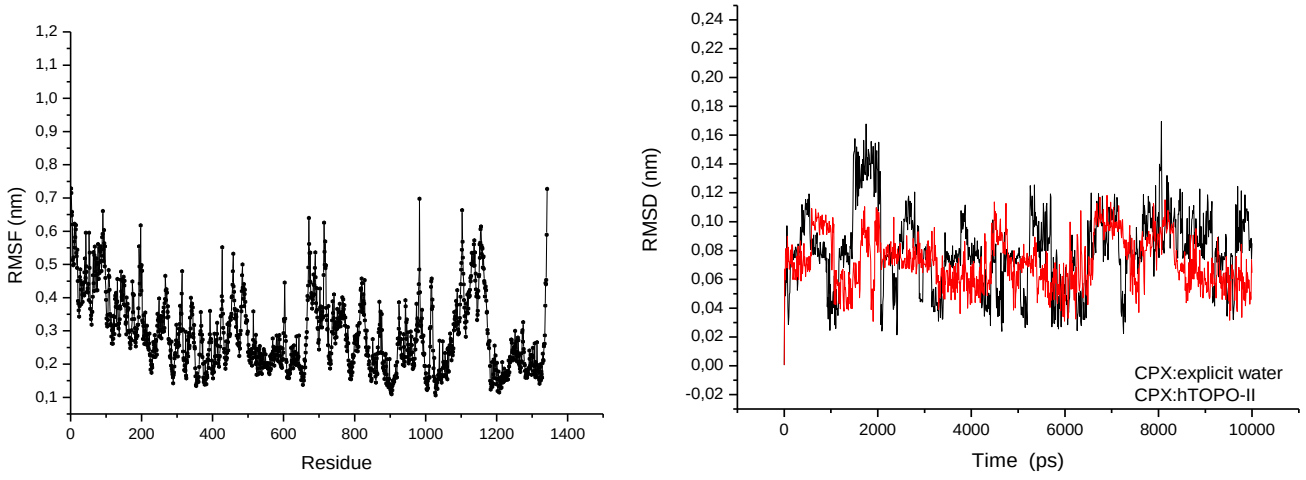

Figure 1. RMSF left and RMSD at right for ciprofloxacin molecule inside the active site (CPX:hTOPO-II) and out of the active site of Topoisomerase-II enzyme (CPX: explicit water).

Figure 1 also shows the Root Mean Square Fluctuation (RMSF). Together with RMSD, the relative RMSF provides information about the fluctuation of each residue in the simulation, with is important to understand the relationship between the flexibility of the residues and the interaction with the ligand, identifying the regions with great flexibility. Generally, the flexibility of the terminal residue and surface loop regions is higher and the protein core is more limited [88]. As can be seen, the fluctuation of residues around 400-600 is more restricted, which can indicate that the CPX forms a stable connection in this region. The total energy variation for CPX in both systems CPX:hTOPO-II and CPX:explicit water were obtained and can be seen in Figure 2 (A and B). As observed, the values remain balanced over the course of the simulation, showing a stabilization of both systems. Regarding the ligand-protein interaction energy, also shown in Figure 2, in the CPX:hTOPO-II system, the total interaction energy average value obtained was equal to -94.27 ± 1.02 kJ.mol^{-1}, which corresponds to the sum of the short-range electrostatic (coulombic) interactions, -36.27 ± 0.77 kJ.mol^{-1}, and the short-range Lennard-Jones interactions, whose average value obtained was equal to -58 ± 0.67 kJ.mol^{-1}.

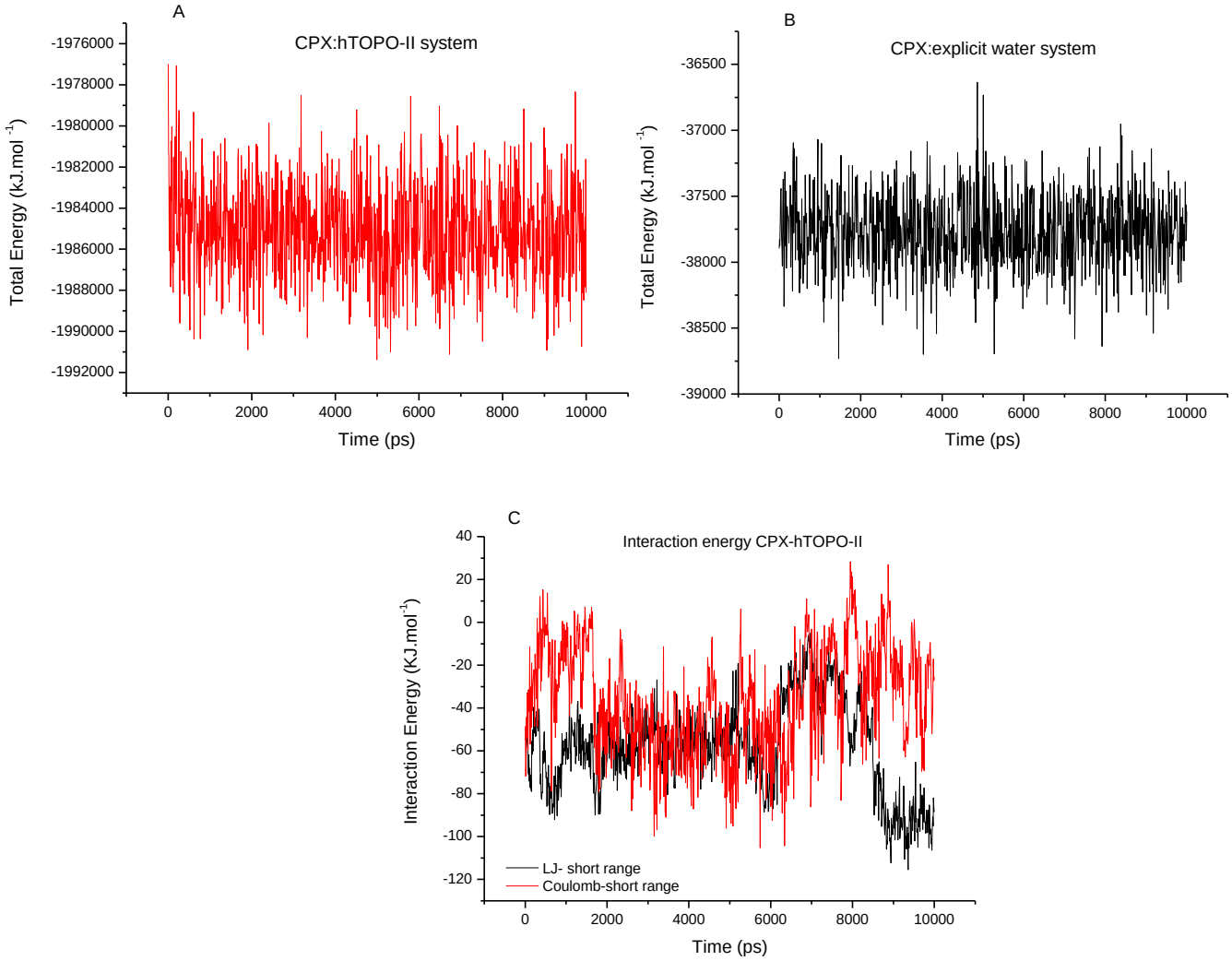

Figure 2. Energy graphs extracted in MD simulations. A and B correspond to the total energy variation for CPX:hTOPO-II and CPX:explicit water system, respectively. C is the interaction energy graph for CPX:hTOPO-II complex. In C, the black line corresponds to Coulombic-type interactions while the red line corresponds to Lennard Jones-type interaction energy.

The hydrogen bonds performed between CPX and hTOPO-II β were the main interactions responsible for the stability of the molecule in the enzyme active site, as showed in Table 1, which contains the main residues that participated in the intermolecular interactions, for the representative conformations selected by OWSCA algorithm. Additionally, the number of hydrogen bonds performed during the MD simulation for all frames can be seen in Figure 3. By analyzing the figure, it can be observed that the CPX shows three hydrogen bonds with hTOPO-IIβ, two of which are quite frequent during most of the simulation time.

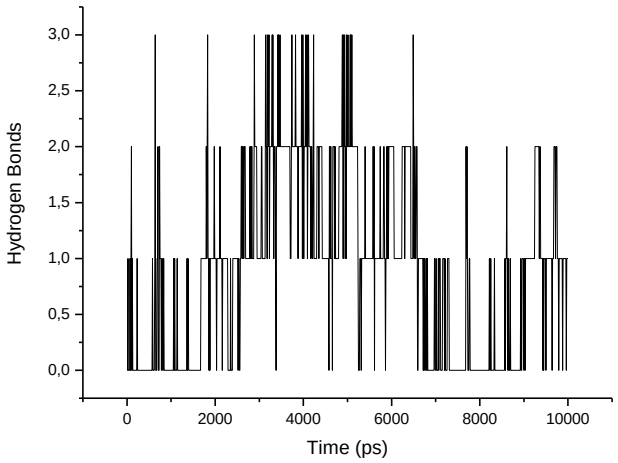

Figure 3. Hydrogen bonds performed between CPX and hTOPO-II βduring the molecular dynamics simulation.

Table 1. Intermolecular interactions performed between human Topoisomerase-II β enzyme and ciprofloxacin molecule during molecular dynamics simulation.

Frame	Time (ps)	Residue	Interaction type
1	2000	Asn 520	HBond
2	2200	Asn 520	HBond
3	2300	Leu 507	HBond
4	2400	Asn 520	HBond
5	2600	Asn 520; Gln 516	HBond
6	3000	Asn 520	HBond
7	3100	Asn 520	HBond
8	3200	Glu 519; Asn 520; Ala 521	HBond
9	3700	Asn 520; Ala 521	HBond
10	3900	Asn 520; Ala 521	HBond
11	4200	Asn 520	HBond
12	4400	Asn 520; Ala 521	HBond
13	4700	Asn 520; Ala 521	HBond
14	5100	Asn 520; Ala 521	HBond

15	5500	Ala 521	HBond
16	7000	-	-
17	7300	Lys 505	π-π; HBond. Electrostatic
18	7500	-	-
19	7700	Arg 503	HBond
20	7900	Arg 503; Lis 505; Gly 504	π-π
21	8000	-	-
22	8250	Lys 505	HBond; π-π
23	8800	-	-
24	9000	Ile 506	HBond
25	9200	Ile 506	HBond
26	9400	Ile 506	HBond
27	9500	-	
28	9800	Ile 506	HBond
29	10000	Ile 506	HBond

Figure 4-A shows the hydrogen bonds performed for frame **8**, at 3200 ps of simulation, which is the time when the greatest number of hydrogen interactions can occur. The residues that participate in the interaction are the Glu 519, Asn 520 and Ala 521. It can also be seen in Figure (4-B), the π-π stacking interactions performed between CPX and amino acids residues Arg 503; Lis 505and Gly 504.

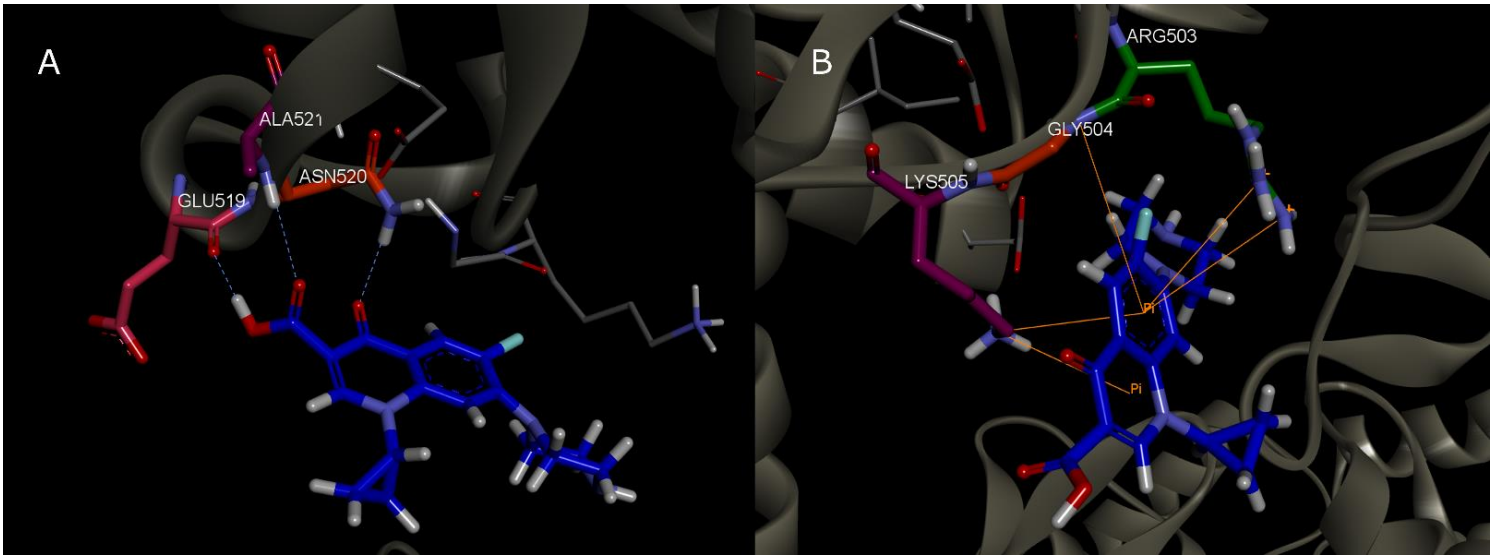

Figure 4. Intermolecular interactions performed during molecular dynamics simulation. A: Hydrogen bonds performed between CPX and the amino acids Glu 519, Asn 520 and Ala 521 at 3200 ps of simulation. B: π-π stacking interactions between CPX and amino acids Arg 503; Lis 505and Glu 504 at 7900 ps of simulation.

In the next step, the chemical shift calculation was performed for the representative configurations in both systems. For the CPX:explicit water system, the first solvation shell was maintained in order to represent the presence of explicit solvent molecules in the NMR calculation. For the CPX:hTOPO-II system, amino acid residues participating in hydrogen interactions with CPX were maintained in order to represent the change in the chemical environment of the molecule inside the active site.

1.1. Spectroscopic parameters: ^{19}F- chemical shifts (δ)

Fluorinated compounds have a wide range of applications, which include anti-inflammatory drugs, anesthesiology, cancer therapy and others. Di- and trifluoromethyl groups can considerably improve the profile of bioactive compounds by increasing their uptake and permeability, as they exhibit unique properties such as high electronegativity, lipophilicity and high steric demand [89]. ^{19}F NMR spectroscopy is a rapidly emerging tool and an attractive alternative for studies of new spectroscopic probes for biological use [90–93]. The main advantages include its high sensitivity, very low background signal, the scarce natural occurrence of fluorinated compounds and the high magnetic moment, the last results in a ^{19}F NMR sensitivity similar to that of ^{1}H [94]. The fluorinated compound chosen for this work is a widely marketed and prescribed antibiotic drug in the world [49,95], which means that CPX is safe for *in vivo* use and that much information related to its pharmacodynamics and pharmacokinetics are already well known [96–98]. The repositioning drug strategy, which consists in proposing new uses for existing drugs [99], is a growing field of research, because the implementation of already known compounds for new applications considerably saves a lot of time and resources related to the studies of bioavailability, toxicity and implementation of these compounds [100–102].

Aiming to investigate if the specific interaction of CPX with hTOPO-IIβ enzyme can be used as a biologic human topoisomerase identifier, theoretical calculations about ^{19}F NMR chemical shifts were performed. Table 2 contains the average of the calculated values for the theoretical ^{19}F NMR shifts in all tested systems. The first point to highlight is the high similarity between the experimental value and the theoretical value obtained for CPX in the CPX:explicit water system. The low Δδ value indicates that the method and the level of theory selected are very accurate for this type of calculation [49]. Secondly, it is observed that the value obtained in the calculation using the implicit solvation model, CPX:implicit water, is very far from the experimental value. It is worth mentioning that results for the system CPX:implicit is similar to values obtained for CPX in vacuum. Such results indicate that explicit solvation is more adequate for representing the solvent effect on CPX. It can also be inferred that the explicit presence of the water molecules in the calculation is important since it creates the proper hydrogen bonding network of water molecules for calculating ^{19}F NMR spectroscopic parameters [103]. As mentioned, the fluorine nucleus has a high sensitivity when compared to the ^{13}C and ^{15}N nuclei, being almost as sensitive as ^{1}H [104]. In this context, although solvent exposure effects can be difficult to observe in nuclei such as ^{13}C and ^{15}N NMR, for the ^{19}F nucleus, solvent-induced isotopic shifts can be as high as 0.25 ppm, offering a very efficient way to probe solvent exposure [105] .

Table 2. Experimental vs. theoretically computed ^{19}F NMR chemical shifts at DFT/B3LYP/aug-cc-pVDZ level for CPX molecule.

System	^{19}F δ_{ppm}	$\Delta\delta_{ppm}$
CPX:Aqueous solution (experimental)	-43.70	0.00
CPX:Explicit water	-43.54	-0.16
CPX:hTOPO-II	-49.73	6.03

CPX:vacuum	-55.11	11.41
CPX:Implicit water	-56.20	12.50

Now, analyzing the effect on the ^{19}F NMR chemical shifts caused by the interaction of CPX with hTOPO-II β (Table 2 and Figures 5 and 6), it is observed that there is a variation of 6.03 ppm in relation to experimental value for CPX in aqueous solution. NMR spectroscopy is a technique extremely sensitive to conformational effects as well as molecular structure effects, both of which can be directly affected by modifications in the chemical environment [106]. Interactions that are able to alter the electronic distribution or even the HOMO-LUMO boundary orbitals can be factors that modify the chemical shift of molecules [107]. By analysis of the figures, it is shown that the interactions of CPX with hTOPO-II caused a modification in the electronic density (figure 6) and the frontier orbitals of CPX (figure 7), which could explain the change in the fluorine chemical shift. This variation in the ^{19}F NMR chemical shift of CPX when it is interacting with the enzyme, represented in Figure 7, can provide important information regarding the occurrence of the ligand in the free form, and in the complexed form with the human topoisomerase-IIβ enzyme. The characteristic signal of CPX when complexed with the enzyme thus constitutes an interesting form of indirect labeling of these proteins, helping to identify their overproduction in the body and consequently in the cancer cell mapping[8,18,85].

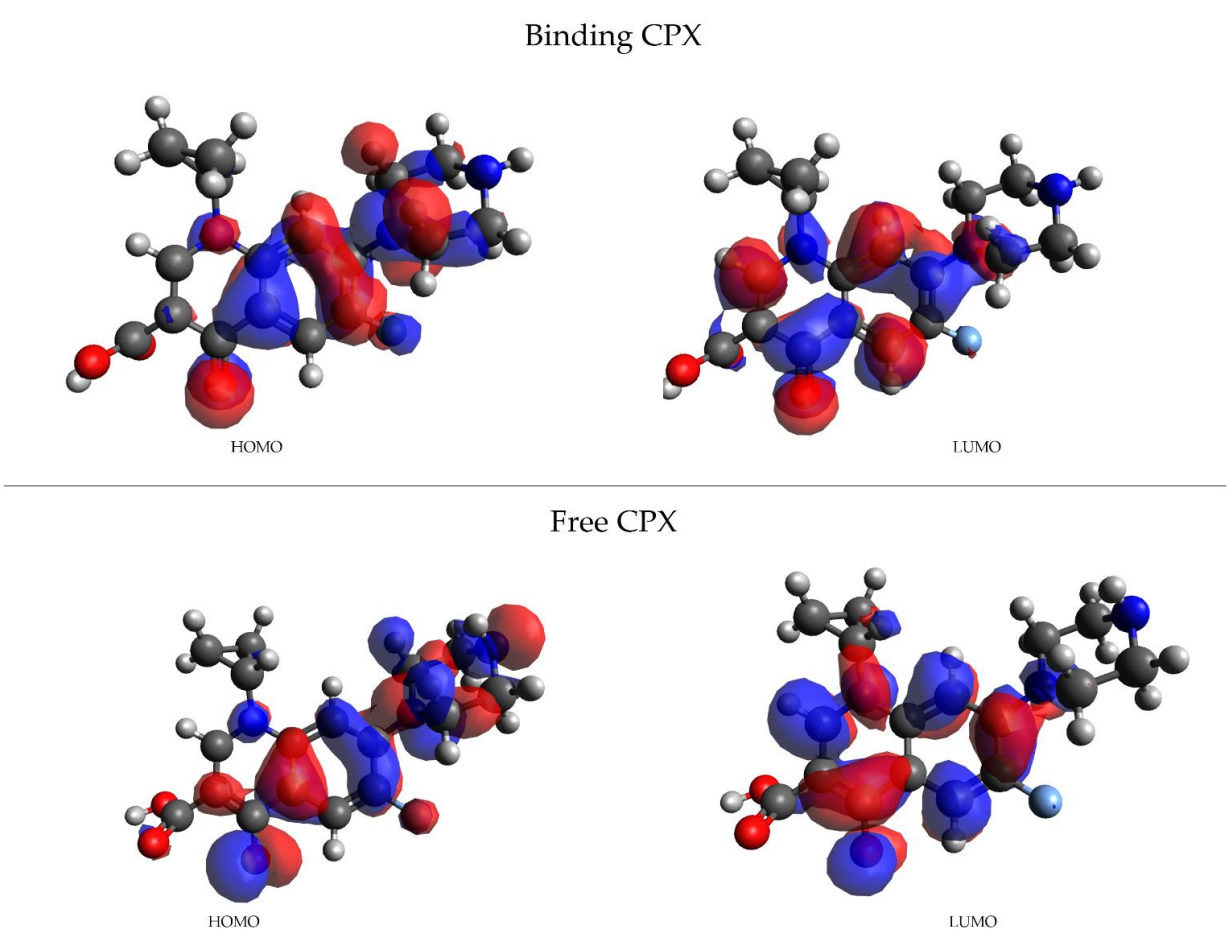

Figure 5. HOMO-LUMO frontier orbital representations for ciprofloxacin molecule in two different environments, in the enzyme active site (binding CPX) and in water (free CPX).

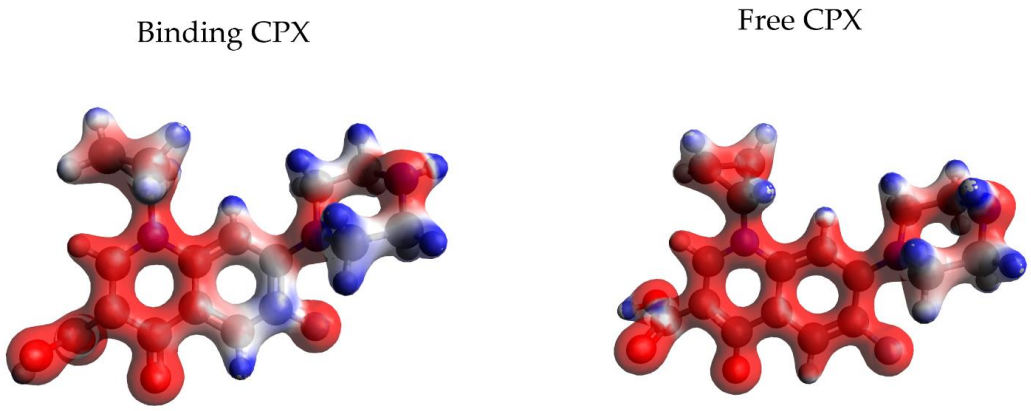

Figure 6. Electronic density variation of ciprofloxacin molecule when it binding to the topoisomerase-II enzyme and in a free form in water solvent.

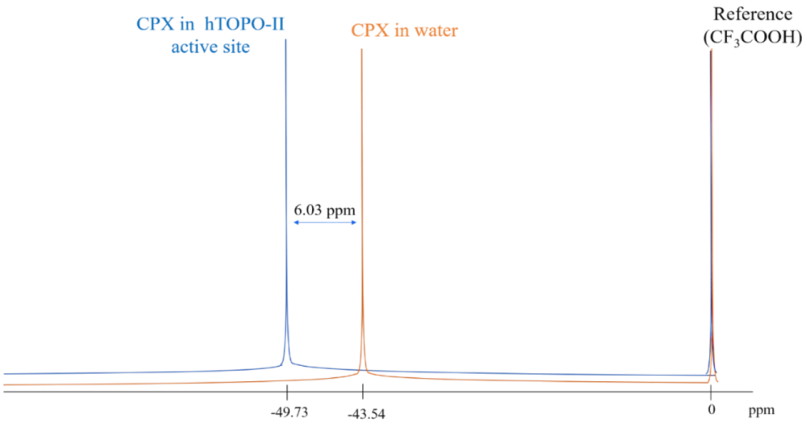

Figure 7. Representation of the variation of the ^{19}F chemical shift for CPX molecule in the hTOPO-II active site.

The results find here point out CPX as a possible candidate for ^{19}F NMR probe, which can be an ally in the cancer diagnosis [29,45]. The application of fluorine probes is advantageous, considering that the natural occurrence of fluorine in biological systems is scarce and the signals from ^{19}F NMR spectroscopy will not find any overlapping background signals to compete with the fluorine probes, making the spectra simpler and easier to analyze [46,47]. Whereas the enzyme concentration in tumor cells is higher [10] and several previous researches have already proven the efficacy of CPX in inhibiting hTOPO-II leading to anti-proliferative and cytotoxic activities of this molecule against several malignant cells [74,108], we can expect that the CPX probe will be efficient and able to reach the desired location. Finally, it is also important to mention that our study is the first attempt to investigate the use of ^{19}F NMR of CPX as a probe for cancer diagnosis, being a starting point for the exploration of this new possibility. From it, new experimental studies must be carried out in order to obtain further informations for the effective implementation of a probe with this proposal.

1. Conclusion

The results found in this work show that the interaction of ciprofloxacin with the human topoisomerase-II β can alter the ^{19}F NMR chemical shift signal of ciprofloxacin, when compared to the same

parameter for the free molecule in water. Thus, this well-known antimicrobial agent constitutes a possible ^{19}F NMR chemical shift probe for cancer diagnosis, capable of indirectly labeling the overexpression of human topoisomerase-IIβ enzyme in the body, and consequently helps in the detection of cancer cells.

Considering the obtained results, and taking in account the low toxicity of this molecule and also that it is an already commercialized drug, ciprofloxacin can be a promising molecule to be used as an ally in cancer diagnosis. We hope our results will stimulate new experimental and full-dimensional theoretical investigations that could assess the validity of this assumption. In fact, our theoretical findings will increase our understanding of the ciprofloxacin and human topoisomerase-II β enzyme and may provide new insights into how it exerts its anti-carcinogenic effect. This would further help in developing new tools for cancer diagnosis.

Author Contributions: Sales, T.A. was responsible for methodology, planning and execution of experiments, data validation and analysis, and writing. Ramalho, T.C. was responsible for supervision, analysis, visualization, data validation, project and resource management, formal analysis and writing review.

Funding: This work was supported Conselho Nacional de Desenvolvimento Científico e Tecnológico (CNPq), Fundação de Amparo ao Ensino e Pesquisa de Minas Gerais (FAPEMIG) and Coordenação de Aperfeiçoamento de Pessoal de Nível Superior/Ministério da Defesa (CAPES/MD) [88882.446445/2019-01]

Acknowledgments: The authors wish to thank the Brazilian financial agencies Conselho Nacional de Desenvolvimento Científico e Tecnológico (CNPq), Fundação de Amparo ao Ensino e Pesquisa de Minas Gerais (FAPEMIG) and Coordenação de Aperfeiçoamento de Pessoal de Nível Superior/Ministério da Defesa (CAPES/MD) for financial support, and the Federal University of Lavras (UFLA) and Minas Gerais State University (UEMG) for providing the physical infrastructure.

Conflicts of Interest: Authors have no conflicts of interest

References

1. Pitman, S.K.; Hoang, U.T.P.; Wi, C.H.; Alsheikh, M.; Hiner, D.A.; Percival, K.M. Revisiting oral fluoroquinolone and multivalent cation drug-drug interactions: Are they still relevant? *Antibiotics* 2019, *8*.
2. Qin, P.; Su, B.; Liu, R. Probing the binding of two fluoroquinolones to lysozyme: a combined spectroscopic and docking study. *Mol. Biosyst.* **2012**, *8*, 1222.
3. Suaifan, G.A.R.Y.; Mohammed, A.A.M. Fluoroquinolones structural and medicinal developments (2013–2018): Where are we now? *Bioorganic Med. Chem.* 2019.
4. Ali, R.; Alminderej, F.M.; Messaoudi, S.; Saleh, S.M. Ratiometric ultrasensitive optical chemisensor film based antibiotic drug for Al(III) and Cu(II) detection. *Talanta* **2021**, *221*.
5. Abdel-Aziz, M.; Park, S.E.; Abuo-Rahma, G.E.D.A.A.; Sayed, M.A.; Kwon, Y. Novel N-4-piperazinyl-ciprofloxacin-chalcone hybrids: Synthesis, physicochemical properties, anticancer and topoisomerase i and II inhibitory activity. *Eur. J. Med. Chem.* **2013**, *69*, 427–438.
6. Majalekar, P.P.; Shirote, P.J. Fluoroquinolones: Blessings Or Curses. *Curr. Drug Targets* **2020**, *21*, 1354–1370.
7. Jacob, D.A.; Mercer, S.L.; Osheroff, N.; Deweese, J.E. Etoposide Quinone Is a Redox-Dependent Topoisomerase II Poison. **2011**, *50*, 5660–5667.
8. Idowu, T.; Schweizer, F. Ubiquitous nature of fluoroquinolones: The oscillation between antibacterial and anticancer activities. *Antibiotics* 2017, *6*.
9. Bisacchi, G.; Hale, M. A "Double-Edged" Scaffold: Antitumor Power within the Antibacterial Quinolone. *Curr. Med. Chem.* **2016**, *23*, 520–577.
10. Heestand, G.M.; Schwaederle, M.; Gatalica, Z.; Arguello, D.; Kurzrock, R. Topoisomerase expression and amplification in solid tumours: Analysis of 24,262 patients. *Eur. J. Cancer* **2017**, *83*, 80–87.
11. Suresh, N.; Suresh, A.; Yerramsetty, S.; Bhadra, M.P.; Alvala, M.; Sekhar, K.V.G.C. Anti-proliferative activity, molecular modeling studies and interaction with calf thymus DNA of novel ciprofloxacin analogues. *J. Chem. Sci.* **2018**, *130*, 1–11.

12. Beberok, A.; Wrześniok, D.; Rok, J.; Rzepka, Z.; Respondek, M.; Buszman, E. Ciprofloxacin triggers the apoptosis of human triple-negative breast cancer MDA-MB-231 cells via the p53/Bax/Bcl-2 signaling pathway. *Int. J. Oncol.* **2018**, *52*, 1727–1737.
13. Chekerov, R.; Klaman, I.; Zafrakas, M.; Könsgen, D.; Mustea, A.; Petschke, B.; Lichtenegger, W.; Sehouli, J.; Dahl, E. Altered Expression Pattern of Topoisomerase IIα in Ovarian Tumor Epithelial and Stromal Cells after Platinum-Based Chemotherapy. *Neoplasia* **2006**, *8*, 38.
14. Faggad, A.; Darb-Esfahani, S.; Wirtz, R.; Sinn, B.; Sehouli, J.; Könsgen, D.; Lage, H.; Weichert, W.; Noske, A.; Budczies, J.; et al. Topoisomerase IIα mRNA and protein expression in ovarian carcinoma: correlation with clinicopathological factors and prognosis. *Mod. Pathol. 2009 224* **2009**, *22*, 579–588.
15. Bai, Y.; Li, L.D.; Li, J.; Lu, X. Targeting of topoisomerases for prognosis and drug resistance in ovarian cancer. *J. Ovarian Res.* **2016**, *9*, 1–12.
16. Zhou, H.; Tang, J.; Zhang, J.; Chen, B.; Kan, J.; Zhang, W.; Zhou, J.; Ma, H. A red lysosome-targeted fluorescent probe for carboxylesterase detection and bioimaging. *J. Mater. Chem. B* **2019**, *7*, 2989–2996.
17. Kirk E. Hevenern; Tatsiana A. Verstak, K.E.L.; Daniel L. Riggsbee, J.W.M. Recent developments in topoisomerase-targeted cancer chemotherapy. *Acta Pharm. Sin. B* **2018**, *8*, 844–861.
18. Cinelli, M.A. Topoisomerase 1B poisons: Over a half-century of drug leads, clinical candidates, and serendipitous discoveries. *Med. Res. Rev.* **2019**, *39*, 1294–1337.
19. Verma, A. Prions, prion-like prionoids, and neurodegenerative disorders. *Ann. Indian Acad. Neurol.* **2016**, *19*, 169–174.
20. Pilleron, S.; Soto-Perez-de-Celis, E.; Vignat, J.; Ferlay, J.; Soerjomataram, I.; Bray, F.; Sarfati, D. Estimated global cancer incidence in the oldest adults in 2018 and projections to 2050. *Int. J. Cancer* **2021**, *148*, 601–608.
21. Dan, N.; Setua, S.; Kashyap, V.; Khan, S.; Jaggi, M.; Yallapu, M.; Chauhan, S.; Dan, N.; Setua, S.; Kashyap, V.K.; et al. Antibody-Drug Conjugates for Cancer Therapy: Chemistry to Clinical Implications. *Pharmaceuticals* **2018**, *11*, 32.
22. Bray, F.; Ferlay, J.; Soerjomataram, I.; Siegel, R.L.; Torre, L.A.; Jemal, A. Global cancer statistics 2018: GLOBOCAN estimates of incidence and mortality worldwide for 36 cancers in 185 countries. **2018**, *68*, 394–424.
23. Kassab, A.E.; Gedawy, E.M. Novel ciprofloxacin hybrids using biology oriented drug synthesis (BIODS) approach: Anticancer activity, effects on cell cycle profile, caspase-3 mediated apoptosis, topoisomerase II inhibition, and antibacterial activity. *Eur. J. Med. Chem.* **2018**, *150*, 403–418.
24. Pashayan, N.; Pharoah, P.D.P. The challenge of early detection in cancer. *Science (80-.).* **2020**, *368*, 589–590.
25. Holtedahl, K. Challenges in early diagnosis of cancer: the fast track. *Scand. J. Prim. Health Care* **2020**, *38*, 251–252.
26. WHO WHO guide for effective programmes: Early detection. *Cancer Control Knowl. into action* **2007**, 3–39.
27. Unger-Saldaña, K. Challenges to the early diagnosis and treatment of breast cancer in developing countries. *World J. Clin. Oncol.* **2014**, *5*, 465.
28. Lue, N.; Kang, J.W.; Yu, C.-C.; Barman, I.; Dingari, N.C.; Feld, M.S.; Dasari, R.R.; Fitzmaurice, M. Portable Optical Fiber Probe-Based Spectroscopic Scanner for Rapid Cancer Diagnosis: A New Tool for Intraoperative Margin Assessment. *PLoS One* **2012**, *7*, e30887.
29. Pereira, B.T.L.L.; Gonçalves, M.A.; Mancini, D.T.; Kuca, K.; Ramalho, T.C. First attempts of the use of 195Pt NMR of phenylbenzothiazole complexes as spectroscopic technique for the cancer diagnosis. *Molecules* **2019**, *24*, 3970.
30. da Rocha, E.P.; Rodrigues, H.A.; da Cunha, E.F.F.; Ramalho, T.C. Probing kinetic and thermodynamic parameters as well as solvent and substituent effects on spectroscopic probes of 2-amino-1,4-naphthoquinone derivatives. *Comput. Theor. Chem.* **2016**, *1096*, 17–26.
31. Wan, X.; Wang, H.; Shi, B.; Guo, Y.; Liu, S.Y.; Wang, X. An enzyme activated fluorescent probe for LTA4H activity sensing and its application in cancer screening. *Talanta* **2023**, *253*, 123887.
32. Zhou, X.; Bai, D.; Yu, H.; Fu, Y.; Song, L.; Wu, Y.; Chen, K.; Li, J.; Yang, Y.; Chen, H.; et al. Detection of rare CTCs by electrochemical biosensor built on quaternary PdPtCuRu nanospheres with mesoporous architectures. *Talanta* **2023**, *253*, 123955.

33. M. Gab Allah, A.; M. Sarhan, A.; M. Elshennawy, N. Edge U-Net: Brain tumor segmentation using MRI based on deep U-Net model with boundary information. *Expert Syst. Appl.* **2023**, *213*, 118833.
34. Kim, J.H.; An, Y.J.; Kim, T.M.; Kim, J.E.; Park, S.; Choi, S.H. Ex vivo NMR metabolomics approach using cerebrospinal fluid for the diagnosis of primary CNS lymphoma: Correlation with MR imaging characteristics. *Cancer Med.* **2022**.
35. Saleem, H.; Maryam, A.; Bokhari, S.A.; Ashiq, A.; Rauf, S.A.; Khalid, R.R.; Qureshi, F.A.; Siddiqi, A.R. Design, synthesis, characterization and computational docking studies of novel sulfonamide derivatives. *EXCLI J.* **2018**, *17*, 169–180.
36. Larkin, J.R.; Anthony, S.; Johanssen, V.A.; Yeo, T.; Sealey, M.; Yates, A.G.; Smith, C.F.; Claridge, T.D.W.; Nicholson, B.D.; Moreland, J.A.; et al. Metabolomic Biomarkers in Blood Samples Identify Cancers in a Mixed Population of Patients with Nonspecific Symptoms. *Clin. Cancer Res.* **2022**, *28*, 1651–1661.
37. Derveaux, E.; Thomeer, M.; Mesotten, L.; Reekmans, G.; Adriaensens, P. Detection of Lung Cancer via Blood Plasma and 1H-NMR Metabolomics: Validation by a Semi-Targeted and Quantitative Approach Using a Protein-Binding Competitor. *Metab. 2021, Vol. 11, Page 537* **2021**, *11*, 537.
38. Kwon, H.N.; Lee, H.; Park, J.W.; Kim, Y.H.; Park, S.; Kim, J.J. Screening for Early Gastric Cancer Using a Noninvasive Urine Metabolomics Approach. *Cancers 2020, Vol. 12, Page 2904* **2020**, *12*, 2904.
39. Michálková, L.; Horník, Š.; Sýkora, J.; Habartová, L.; Setnička, V. Diagnosis of pancreatic cancer via1H NMR metabolomics of human plasma. *Analyst* **2018**, *143*, 5974–5978.
40. Mikkonen, J.J.W.; Singh, S.P.; Akhi, R.; Salo, T.; Lappalainen, R.; González-Arriagada, W.A.; Lopes, M.A.; Kullaa, A.M.; Myllymaa, S. Potential role of nuclear magnetic resonance spectroscopy to identify salivary metabolite alterations in patients with head and neck cancer. *Oncol. Lett.* **2018**, *16*, 6795–6800.
41. Erben, V.; Bhardwaj, M.; Schrotz-King, P.; Brenner, H. Metabolomics Biomarkers for Detection of Colorectal Neoplasms: A Systematic Review. *Cancers 2018, Vol. 10, Page 246* **2018**, *10*, 246.
42. Yang, B.; Liao, G. qiang; Wen, X. fei; Chen, W. hua; Cheng, S.; Stolzenburg, J.U.; Ganzer, R.; Neuhaus, J. Nuclear magnetic resonance spectroscopy as a new approach for improvement of early diagnosis and risk stratification of prostate cancer. *J. Zhejiang Univ. B 2017 1811* **2017**, *18*, 921–933.
43. Tang, Z.-Y.; Zhang, Y.; Chen, Y.-T.; Yu, Q.; An, L.-K. The first small fluorescent probe as Tyrosyl-DNA phosphodiesterase 1 (TDP1) substrate. *Dye. Pigment.* **2019**, *169*, 45–50.
44. Zhou, J.; Ma, H. Design principles of spectroscopic probes for biological applications. *Chem. Sci.* **2016**, *7*, 6309–6315.
45. Stanley, P.D. Principles and Topical Applications of 19F NMR Spectrometry. *Organofluorines* **2002**, 1–61.
46. Marsh, E.N.G.; Suzuki, Y. Using 19F NMR to Probe Biological Interactions of Proteins and Peptides. *ACS Chem. Biol.* **2014**, *9*, 1242–1250.
47. Gimenez, D.; Phelan, A.; Murphy, C.D.; Cobb, S.L. 19F NMR as a tool in chemical biology. *Beilstein J. Org. Chem. 1728* **2021**, *17*, 293–318.
48. Jawaria, R.; Hussain, M.; Khalid, M.; Khan, M.U.; Tahir, M.N.; Naseer, M.M.; Braga, A.A.C.; Shafiq, Z. Synthesis, crystal structure analysis, spectral characterization and nonlinear optical exploration of potent thiosemicarbazones based compounds: A DFT refine experimental study. *Inorganica Chim. Acta* **2019**, *486*, 162–171.
49. Koch, A.; Stamboliyska, B.; Mikhova, B.; Breznica-Selmani, P.; Mladenovska, K.; Popovski, E. Calculations of 13C NMR chemical shifts and F–C coupling constants of ciprofloxacin. *Magn. Reson. Chem.* **2019**, *57*, S75–S84.
50. Ghosh, D.; Rhodes, S.; Winder, D.; Atkinson, A.; Gibson, J.; Ming, W.; Padgett, C.; Landge, S.; Aiken, K. Spectroscopic investigation of bis-appended 1,2,3-triazole probe for the detection of Cu(II) ion. *J. Mol. Struct.* **2017**, *1134*, 638–648.
51. Ramalho, T.C.; Taft, C.A. Thermal and solvent effects on the NMR and UV parameters of some bioreductive drugs. *J. Chem. Phys.* **2005**,

123, 054319.

52. Pudipeddi, A.; Vasudevan, S.; Shanmugam, K.; Mohan S, S.; Vairaprakash, P.; Neelakantan, P.; Balraj, A.S.; Solomon, A.P. Design, dynamic docking, synthesis, and in vitro validation of a novel DNA gyrase B inhibitor. *J. Biomol. Struct. Dyn.* **2022**, *4*, 1–14.
53. Khan, T.; Sankhe, K.; Suvarna, V.; Sherje, A.; Patel, K.; Dravyakar, B. DNA gyrase inhibitors: Progress and synthesis of potent compounds as antibacterial agents. *Biomed. Pharmacother.* **2018**, *103*, 923–938.
54. Berman, H.M.; Westbrook, J.; Feng, Z.; Gilliland, G.; Bhat, T.N.; Weissig, H.; Shindyalov, I.N.; Bourne, P.E. The Protein Data Bank. *Nucleic Acids Res.* **2000**, *28*, 235–42.
55. Malde, A.K.; Zuo, L.; Breeze, M.; Stroet, M.; Poger, D.; Nair, P.C.; Oostenbrink, C.; Mark, A.E. An Automated force field Topology Builder (ATB) and repository: Version 1.0. *J. Chem. Theory Comput.* **2011**, *7*, 4026–4037.
56. Abraham, M.J.; Murtola, T.; Schulz, R.; Páll, S.; Smith, J.C.; Hess, B.; Lindah, E. Gromacs: High performance molecular simulations through multi-level parallelism from laptops to supercomputers. *SoftwareX* **2015**, *1–2*, 19–25.
57. Christen, M.; Hünenberger, P.H.; Bakowies, D.; Baron, R.; Bürgi, R.; Geerke, D.P.; Heinz, T.N.; Kastenholz, M.A.; Kräutler, V.; Oostenbrink, C.; et al. The GROMOS software for biomolecular simulation: GROMOS05. *J. Comput. Chem.* **2005**, *26*, 1719–1751.
58. Gonçalves, M.A.; Santos, L.S.; Prata, D.M.; Peixoto, F.C.; da Cunha, E.F.F.; Ramalho, T.C. Optimal wavelet signal compression as an efficient alternative to investigate molecular dynamics simulations: application to thermal and solvent effects of MRI probes. *Theor. Chem. Acc.* **2017**, *136*, 15.
59. M. J. Frisch, G. W. Trucks, H. B. Schlegel, G. E. Scuseria, M. A. Robb, J. R. Cheeseman, G. Scalmani, V. Barone, B. Mennucci, G. A. Petersson, H. Nakatsuji, M. Caricato, X. Li, H. P. Hratchian, A. F. Izmaylov, J. Bloino, G. Zheng, J. L. Sonnenberg, M. Had, and D.J.F. *Gaussian 09*; Gaussian, Inc., Wallingford CT, 2009;
60. Jr., T.H.D. Gaussian basis sets for use in correlated molecular calculations. I. The atoms boron through neon and hydrogen. *J. Chem. Phys.* **1998**, *90*, 1007.
61. Kendall, R.A.; Jr., T.H.D.; Harrison, R.J. Electron affinities of the first-row atoms revisited. Systematic basis sets and wave functions. *J. Chem. Phys.* **1998**, *96*, 6796.
62. Woon, D.E.; Jr., T.H.D. Gaussian basis sets for use in correlated molecular calculations. III. The atoms aluminum through argon. *J. Chem. Phys.* **1998**, *98*, 1358.
63. Wolinski, K.; Hinton, J.F.; Pulay, P. Efficient implementation of the gauge-independent atomic orbital method for NMR chemical shift calculations. *J. Am. Chem. Soc.* **2002**, *112*, 8251–8260.
64. Mejía-Urueta, R.; Mestre-Quintero, K.; Vivas-Reyes, R. DFT-GIAO Calculation of Properties of 19 F NMR and Stability Study of Environmentally Relevant Perfluoroalkylsulfonamides (PFASAmide). *Artic. J. Braz. Chem. Soc* **2268**, *22*.
65. Dapprich, S.; Komáromi, I.; Byun, K.S.; Morokuma, K.; Frisch, M.J. A new ONIOM implementation in Gaussian98. Part I. The calculation of energies, gradients, vibrational frequencies and electric field derivatives. *J. Mol. Struct. THEOCHEM* **1999**, *461–462*, 1–21.
66. Marenich, A. V; Cramer, C.J.; Truhlar, D.G. Universal Solvation Model Based on Solute Electron Density and on a Continuum Model of the Solvent Defined by the Bulk Dielectric Constant and Atomic Surface Tensions.
67. Trefi, S.; Gilard, V.; Malet-Martino, M.; Martino, R. Generic ciprofloxacin tablets contain the stated amount of drug and different impurity profiles: A 19F, 1H and DOSY NMR analysis. *J. Pharm. Biomed. Anal.* **2007**, *44*, 743–754.
68. Zhang, F.-F.; Jiang, M.-H.; Sun, L.-L.; Zheng, F.; Dong, L.; Shah, V.; Shen, W.-B.; Ding, Y. Quantitative analysis of sitagliptin using the ^{19}F-NMR method: a universal technique for fluorinated compound detection. *Analyst* **2015**, *140*, 280–286.
69. Ezelarab, H.A.A.; Abbas, S.H.; Hassan, H.A.; Abuo-Rahma, G.E.D.A. Recent updates of fluoroquinolones as antibacterial agents. *Arch. Pharm. (Weinheim).* 2018, *351*.
70. Fief, C.A.; Hoang, K.G.; Phipps, S.D.; Wallace, J.L.; Deweese, J.E. Examining the Impact of Antimicrobial Fluoroquinolones on Human

DNA Topoisomerase IIα and IIβ. *ACS Omega* **2019**, *4*, 4049–4055.

71. Beberok, A.; Wrześniok, D.; Minecka, A.; Rok, J.; Delijewski, M.; Rzepka, Z.; Respondek, M.; Buszman, E. Ciprofloxacin-mediated induction of S-phase cell cycle arrest and apoptosis in COLO829 melanoma cells. *Pharmacol. Reports* **2018**, *70*, 6–13.
72. Perrone, C.E.; Takahashi, K.C.; Williams, G.M. Inhibition of human topoisomerase IIα by fluoroquinolones and ultraviolet A irradiation. *Toxicol. Sci.* **2002**, *69*, 16–22.
73. Swedan, H.K.; Kassab, A.E.; Gedawy, E.M.; Elmeligie, S.E. Design, synthesis, and biological evaluation of novel ciprofloxacin derivatives as potential anticancer agents targeting topoisomerase II enzyme. *J. Enzyme Inhib. Med. Chem.* **2023**, *38*, 118–137.
74. Mazandaran, K.E.; Mirshokraee, S.A.; Didehban, K.; Houshdar Tehrani, M.H. Design, Synthesis and Biological Evaluation of Ciprofloxacin- Peptide Conjugates as Anticancer Agents. *Iran. J. Pharm. Res. IJPR* **2019**, *18*, 1823.
75. Mohammed, H.H.H.; Abd El-Hafeez, A.A.; Ebeid, K.; Mekkawy, A.I.; Abourehab, M.A.S.; Wafa, E.I.; Alhaj-Suliman, S.O.; Salem, A.K.; Ghosh, P.; Abuo-Rahma, G.E.D.A.; et al. New 1,2,3-triazole linked ciprofloxacin-chalcones induce DNA damage by inhibiting human topoisomerase I& II and tubulin polymerization. *J. Enzyme Inhib. Med. Chem.* **2022**, *37*, 1346–1363.
76. Mohammed, H.H.H.; Abbas, S.H.; Hayallah, A.M.; Abuo-Rahma, G.E.D.A.; Mostafa, Y.A. Novel urea linked ciprofloxacin-chalcone hybrids having antiproliferative topoisomerases I/II inhibitory activities and caspases-mediated apoptosis. *Bioorg. Chem.* **2021**, *106*, 104422.
77. Sales, T.A.; Ramalho, T.C. Ciprofloxacin/Topoisomerase-II complex as a promising dual UV–Vis/fluorescent probe: accomplishments and opportunities for the cancer diagnosis. *Theor. Chem. Acc.* **2022**, *141*, 1–10.
78. Cowen, T.; Karim, K.; Piletsky, S. No Title. *Anal. Chim. Acta* **2016**, *936*, 62–74.
79. Jadhav, A.K.; Karuppayil, S.M. Molecular docking studies on thirteen fluoroquinolines with human topoisomerase II a and b. *Silico Pharmacol.* **2017**, *5*.
80. Patel, J.R.; Joshi, H. V.; Shah, U.A.; Patel, J.K. A Review on Computational Software Tools for Drug Design and Discovery. *Indo Glob. J. Pharm. Sci.* **2022**, *12*, 53–81.
81. Pajeva, I.; Tsakovska, I.; Pencheva, T.; Alov, P.; Al Sharif, M.; Lessigiarska, I.; Jereva, D.; Diukendjieva, A. In silico Studies of Biologically Active Molecules. *Stud. Comput. Intell.* **2021**, *934*, 421–451.
82. Caballero, J. The latest automated docking technologies for novel drug discovery. *Expert Opin. Drug Discov.* **2020**, *16*, 625–645.
83. Frye, L.; Bhat, S.; Akinsanya, K.; Abel, R. From computer-aided drug discovery to computer-driven drug discovery. *Drug Discov. Today Technol.* **2021**, *39*, 111–117.
84. Shukla, R.; Tripathi, T. Molecular Dynamics Simulation in Drug Discovery: Opportunities and Challenges. *Innov. Implementations Comput. Aided Drug Discov. Strateg. Ration. Drug Des.* **2021**, 295–316.
85. McClendon, A.K.; Osheroff, N. DNA Topoisomerase II, Genotoxicity, and Cancer. *Mutat. Res. Mol. Mech. Mutagen.* **2007**, *623*, 83–97.
86. Sales, T.A.; Marcussi, S.; da Cunha, E.F.F.; Kuca, K.; Ramalho, T.C. Can inhibitors of snake venom phospholipases A<inf>2</inf> lead to new insights into anti-inflammatory therapy in humans? A theoretical study. *Toxins (Basel).* **2017**, *9*.
87. Schreiner, W.; Karch, R.; Knapp, B.; Ilieva, N. Relaxation estimation of RMSD in molecular dynamics immunosimulations. *Comput. Math. Methods Med.* **2012**, *2012*.
88. Bhardwaj, P.; Biswas, G.P.; Mahata, N.; Ghanta, S.; Bhunia, B. Exploration of binding mechanism of triclosan towards cancer markers using molecular docking and molecular dynamics. *Chemosphere* **2022**, *293*.
89. Chekmenev, E.Y.; Chow, S.K.; Tofan, D.; Weitekamp, D.P.; Ross, B.D.; Bhattacharya, P. Fluorine-19 NMR chemical shift probes molecular binding to lipid membranes. *J. Phys. Chem. B* **2008**, *112*, 6285–6287.
90. Maxwell, R.J.; Workman, P.; Griffiths, J.R. Demonstration of tumor-selective retention of fluorinated nitroimidazole probes by 19F magnetic resonance spectroscopy in vivo. *Int. J. Radiat. Oncol.* **1989**, *16*, 925–929.

91. Peterson, K.L.; Srivastava, K.; Pierre, V.C. Fluorinated paramagnetic complexes: Sensitive and responsive probes for magnetic resonance spectroscopy and imaging. *Front. Chem.* 2018, *6*.

92. Ojugo, A.S.E.; Mcsheehy, P.M.J.; Mcintyre, D.J.O.; Mccoy, C.; Stubbs, M.; Leach, M.O.; Judson, I.R.; Grif®ths, J.R. Measurement of the extracellular pH of solid tumours in mice by magnetic resonance spectroscopy: a comparison of exogenous 19 F and 31 P probes. **1999**.

93. Ye, Y.; Liu, X.; Zhang, Z.; Wu, Q.; Jiang, B.; Jiang, L.; Zhang, X.; Liu, M.; Pielak, G.J.; Li, C. 19F NMR Spectroscopy as a Probe of Cytoplasmic Viscosity and Weak Protein Interactions in Living Cells. *Chem. – A Eur. J.* **2013**, *19*, 12705–12710.

94. Ulrich, A.S. Solid state 19F NMR methods for studying biomembranes. *Prog. Nucl. Magn. Reson. Spectrosc.* **2005**, *46*, 1–21.

95. Cdc, R. *Outpatient Antibiotic Prescriptions — United States, 2017*; 2017;

96. Crump, B.; Wise, R.; Dent, J. Pharmacokinetics and tissue penetration of ciprofloxacin. *Antimicrob. Agents Chemother.* **1983**, *24*, 784–786.

97. Brunner, M.; Staß, H.; Möller, J.G.; Schrolnberger, C.; Erovic, B.; Hollenstein, U.; Zeitlinger, M.; Georg Eichler, H.; Müller, M. Target Site Concentrations of Ciprofloxacin after Single Intravenous and Oral Doses. *Antimicrob. Agents Chemother.* **2002**, *46*, 3724.

98. Yuan, F.; Hu, C.; Hu, X.; Wei, D.; Chen, Y.; Qu, J. Photodegradation and toxicity changes of antibiotics in UV and UV/H2O2 process. *J. Hazard. Mater.* **2011**, *185*, 1256–1263.

99. Ashburn, T.T.; Thor, K.B. Drug repositioning: identifying and developing new uses for existing drugs. *Nat. Rev. Drug Discov.* **2004**, *3*, 673–683.

100. Mucke, H.A. The case of galantamine: repurposing and late blooming of a cholinergic drug. *Futur. Sci. OA* **2015**, *1*, fso.15.73.

101. Mullard, A. Drug repurposing programmes get lift off. *Nat. Rev. Drug Discov.* **2012**, *11*, 505–506.

102. Durães, F.; Pinto, M.; Sousa, E.; Durães, F.; Pinto, M.; Sousa, E. Old Drugs as New Treatments for Neurodegenerative Diseases. *Pharmaceuticals* **2018**, *11*, 44.

103. and, E.Y.L.; Gerig*, J.T. Origins of Fluorine NMR Chemical Shifts in Fluorine-Containing Proteins†. *J. Am. Chem. Soc.* **2000**, *122*, 4408–4417.

104. Modo, M. 19F Magnetic Resonance Imaging and Spectroscopy in Neuroscience. *Neuroscience* **2021**.

105. Evanics, F.; Kitevski, J.L.; Bezsonova, I.; Forman-Kay, J.; Prosser, R.S. 19F NMR studies of solvent exposure and peptide binding to an SH3 domain. *Biochim. Biophys. Acta - Gen. Subj.* **2007**, *1770*, 221–230.

106. Gonçalves, M.A.; Gonçalves, A.S.; Franca, T.C.C.; Santana, M.S.; da Cunha, E.F.F.; Ramalho, T.C. Improved Protocol for the Selection of Structures from Molecular Dynamics of Organic Systems in Solution: The Value of Investigating Different Wavelet Families. *J. Chem. Theory Comput.* **2022**.

107. Rayene, K.; Imane, D.; Abdelaziz, B.; Leila, N.; Fatiha, M.; Abdelkrim, G.; Bouzid, G.; Ismahan, L.; Brahim, H.; Rabah, O. Molecular modeling study of structures, Hirschfield surface, NBO, AIM, RDG, IGM and 1HNMR of thymoquinone/hydroxypropyl-β-cyclodextrin inclusion complex from QM calculations. *J. Mol. Struct.* **2022**, *1249*, 131565.

108. Jaber, D.F.; Jallad, M.A.N.; Abdelnoor, A.M. The effect of ciprofloxacin on the growth of B16F10 melanoma cells. *J. Cancer Res. Ther.* **2017**, *13*, 956–960.